

## ORIGINAL ARTICLE

# Population Pharmacokinetics Modeling of Unbound Efavirenz, Atazanavir, and Ritonavir in HIV-Infected Subjects With Aging Biomarkers

JB Dumond<sup>1\*</sup>, J Chen<sup>1</sup>, M Cottrell<sup>1</sup>, CR Trezza<sup>1</sup>, HMA Prince<sup>2</sup>, C Sykes<sup>1</sup>, C Torrice<sup>3</sup>, N White<sup>1</sup>, S Malone<sup>1</sup>, R Wang<sup>1</sup>, KB Patterson<sup>2</sup>, NE Sharpless<sup>3</sup> and A Forrest<sup>1</sup>

Unbound drug is the pharmacodynamically relevant concentration. This study aimed to determine if chronologic age or markers of biologic aging, such as the frailty phenotype and p16<sup>INK4a</sup> gene expression, altered unbound pharmacokinetics (PKs) of efavirenz (EFV) and atazanavir/ritonavir (ATV/RTV). Sixty human immunodeficiency virus (HIV)-infected participants receiving EFV and 31 receiving ATV/RTV provided 1 to 11 samples to quantify total and unbound plasma concentrations. Population PK models with total and unbound concentrations simultaneously described are developed for each drug. The unbound fractions for EFV, ATV, and RTV are 0.65%, 5.67%, and 0.63%, respectively. Covariate analysis suggests RTV unbound PK is sensitive to body size; unbound fraction of RTV is 34% lower with body mass index (BMI) above 30 kg/m<sup>2</sup>. No alterations in drug clearance or unbound fraction with age, frailty, or p16<sup>INK4a</sup> expression were observed. Assessing functional and physiologic aging markers to inform potential PK changes is necessary to determine if drug/dosing changes are warranted in the aging population.

*CPT Pharmacometrics Syst. Pharmacol.* (2017) 6, 128–135; doi:10.1002/psp4.12151; published online 29 December 2016.

## Study Highlights

### WHAT IS THE CURRENT KNOWLEDGE ON THE TOPIC?

☑ The physiology of aging is well described, but inconsistently translated in the literature to changes in PK. HIV-infected patients rely on ARV therapy with complex ADMET profiles to control their disease, and this population is aging with little knowledge of how aging processes affect ARVs.

### WHAT QUESTION DID THIS STUDY ADDRESS?

☑ This study asked whether aging, chronologic, immunologic, or functional, alters disposition of the unbound EFV, ATV, and RTV.

### WHAT THIS STUDY ADDS TO OUR KNOWLEDGE

☑ This study demonstrates that aging processes do not appear to impact unbound drug disposition for these three agents, and dosage adjustments to improve efficacy or decrease toxicity are unlikely to be warranted.

### HOW MIGHT THIS CHANGE DRUG DISCOVERY, DEVELOPMENT, AND/OR THERAPEUTICS?

☑ Quantifying the effects of aging on PK/pharmacodynamics is difficult and should include other markers of aging that reflect biology and physiology rather than chronologic age alone.

As humans age, declines in renal and hepatic function are well-described.<sup>1</sup> Less straightforward, however, are the impacts of these changes in physiology on drug metabolism, transport, and elimination. For drugs that undergo mainly renal elimination, dosing can be guided by changes in serum creatinine, an easily assessed marker of renal function. For drugs with hepatic elimination, the effects of aging on phase I and phase II metabolism and transport are not easily quantified in order to guide drug therapy. Potential changes in protein binding are not thought to be of major clinical significance in most cases,<sup>2</sup> but changes in the intrinsic clearance of unbound drug can further complicate pharmacotherapy in the elderly.<sup>3</sup>

Current US Department of Health and Human Services antiretroviral (ARV) treatment guidelines recommend treating all human immunodeficiency virus (HIV)-infected patients regardless of CD4 T-cell count, and especially

those patients ages 50 years and older.<sup>4</sup> The advent of well-tolerated, highly effective ARVs has partially contributed to the increased proportion of patients living with HIV who are in this age range, considered “old” in the HIV treatment community for a variety of immunologic and functional reasons.<sup>5</sup> Half of the HIV-infected population in the United States is currently 50 years or older, with the age distribution concentrated between 50 and 65 years of age.<sup>6</sup> HIV treatment, as it stands currently, is life-long. Many ARVs have complex disposition profiles,<sup>4</sup> with unknown effects of aging on their pharmacokinetics (PKs). To probe potential changes in disposition, three ARVs used in two different regimens with key disposition characteristics were selected for study: efavirenz (EFV) and atazanavir/ritonavir (ATV/RTV; co-administered with tenofovir and emtricitabine, reported separately).

<sup>1</sup>UNC Eshelman School of Pharmacy, University of North Carolina at Chapel Hill, Chapel Hill, North Carolina, USA; <sup>2</sup>School of Medicine, University of North Carolina at Chapel Hill, Chapel Hill, North Carolina, USA; <sup>3</sup>Lineberger Comprehensive Cancer Center, University of North Carolina at Chapel Hill, Chapel Hill, North Carolina, USA.

\*Correspondence: JB Dumond ([jdumond@unc.edu](mailto:jdumond@unc.edu))

Received 13 May 2016; accepted 19 October 2016; published online on 29 December 2016. doi:10.1002/psp4.12151

ATV (coadministered with RTV) was chosen to probe absorption, as its absorption requires an acidic gastric environment,<sup>7</sup> and older patients may have changes in gastric pH.

As body water decreases with age, and body fat increases, lipophilic drugs display increased volumes of distribution,<sup>8</sup> whereas polar drugs display decreased volumes of distribution.<sup>9</sup> As ATV, RTV, and EFV are all lipophilic,<sup>7,10,11</sup> volume of distribution may increase with aging. Additionally, these drugs are all substrates of phase I cytochrome P 450 enzymes; ATV and RTV are substrates and inhibitors of CYP3A,<sup>12</sup> whereas EFV is a substrate and inducer of CYP3A and CYP2B6.<sup>10</sup> RTV displays a complex, dose-dependent CYP450 metabolic pattern.<sup>11</sup> ATV also inhibits UGT1A1 activity.<sup>12</sup> Altered drug metabolism may occur with aging, as liver mass and blood flow decrease 20–50%, and cytochrome P450 enzyme metabolism may decrease up to 25%.<sup>13–16</sup> In addition to metabolism, all three drugs are substrates, inhibitors, and inducers of several efflux transporters and inhibitors of several uptake transporters (reviewed in ref. 17); transporter expression may be affected by aging.<sup>18</sup>

As laid out in Schoen *et al.*,<sup>19</sup> it is hypothesized that offsetting changes in intrinsic clearance due to altered metabolism and unbound fraction of a drug highly bound to albumin could result in unchanged total oral clearance and similar total plasma concentrations in older patients, but with significant increases in unbound concentrations. EFV, ATV, and RTV are >99.5%,<sup>10</sup> 98–99%, and 86%<sup>12</sup> bound to plasma proteins, respectively. EFV is mainly bound to albumin, whereas ATV and RTV are mainly bound to alpha-1 acid glycoprotein, and were chosen to test the hypothesis presented in the Schoen *et al.*<sup>19</sup> review. Others have also proposed that for highly protein-bound, capacity-limited drugs, measuring total drug alone may mask important changes in intrinsic, unbound drug clearance in the elderly; this has been demonstrated for valproic acid, and suggested for phenytoin and diazepam (reviewed in ref. 3).

Syndromes of aging and the heterogeneity of the aging process itself further complicate the quantification of the effects of physiologic processes on PK, and the geriatric field has several ways of trying to capture this heterogeneity. Frailty is described as a clinical syndrome of decreased functional reserves that increases morbidity and mortality, thought to be a result of altered biochemical processes in the body that result in increased inflammation. A characteristic phenotype has been described<sup>20</sup> and applied to the HIV population, which demonstrates occurrence of this phenotype at ages 10 years younger than uninfected controls.<sup>21</sup> Significant decreases in drug clearance of 50% or greater have been demonstrated in the frail HIV-negative elderly for acetaminophen,<sup>22</sup> metoclopramide,<sup>23</sup> and antipyrene<sup>24</sup> compared with younger, healthier, HIV-negative subjects. This increase in exposure is likely due to a combination of decreased renal clearance and cytokine-induced downregulation of metabolic enzymes.<sup>25</sup>

The p16<sup>INK4a</sup> tumor suppressor-gene expression in peripheral blood T lymphocyte cellular fractions is a marker of cellular senescence that correlates with both chronologic age and inflammatory state, validated in both healthy

volunteers<sup>26</sup> and HIV-infected patients.<sup>27</sup> In untreated, viremic HIV-infected patients this correlation was not seen, suggesting that the inflammatory state induced by viremia alters p16<sup>INK4a</sup> expression patterns. In treated patients with suppressed virus, p16<sup>INK4a</sup> expression were similar to uninfected controls and correlated with chronologic age, demonstrating that it can be used as a marker of cellular aging and senescence in this population.

As HIV-infected patients may develop frailty discordant from their chronological age, functional and biochemical surrogates of an aging immune system are critical to describe interactions between the aging process and ARV PK. Here, nonlinear mixed effects modeling was used to assess unbound drug PKs in HIV-infected subjects ranging in age from 20 to 73 years who underwent such assessments for a covariate analysis that reflects the biology of aging.

## METHODS

### Clinical study conduct

HIV-infected adults ( $\geq 18$  years old) receiving EFV 600 mg or ATV/RTV 300/100 mg once daily for  $\geq 2$  weeks were recruited from the UNC HealthCare Infectious Diseases Clinic (Chapel Hill, NC) and the Cone Health Regional Center for Infectious Diseases (Greensboro, NC). All subjects also received tenofovir/emtricitabine 300/200 mg once daily in their HIV regimen with the drug of interest. The study protocol was approved by the UNC Biomedical Institutional Review Board, as well as the Moses Cone Hospital Institutional Review Board (Clinicaltrials.gov NCT01180075).

Subjects were recruited for two separate sampling groups, sparse and intensive. Following a screening visit to assess medication adherence and medical history, participants provided blood samples at four time points (predose, and then 2 hours, 4–6 hours, and 10–14 hours postdose) or 11 time points. Sparse sampling times were optimized based on the intensive PK study; detailed descriptions of methods and results for this group have been published.<sup>28</sup> Briefly, to optimize collection times, a two-compartment model with first-order absorption and linear clearance was fit to each drug using S-ADAPT with the S-ADAPT TRAN pre- and postprocessing package.<sup>29</sup> The mean parameter estimates and their variability were used in designing the sampling scheme. D-optimal sampling design (ADAPT5; Biomedical Simulations Resource, University of California at Los Angeles, Los Angeles, CA) was used to select windows of sampling times practical and feasible for study conduct, optimizing the clearance for each drug. For each drug, four optimal times were selected, and then times were aligned as closely as possible for each drug in the regimen (tenofovir, emtricitabine, and efavirenz; or tenofovir, emtricitabine, atazanavir, and ritonavir) in order to capture informative regions of the PK profiles. The optimal times aligned so one scheme could be used regardless of regimen. Power calculations, using a two-sided test with a significance level of 0.05, for a regression analysis of age effects on drug clearance, a sample size of 36 provides ability to detect a correlation of 0.55 (30% variation) with

90% power; a sample size of 28 would provide 80% power to detect the same difference.

At each sampling time, subjects provided blood for total and unbound drug concentrations. At one visit, subjects underwent frailty phenotyping and provided additional blood for pharmacogenomics, cytokine concentrations, and p16<sup>INK4a</sup> expression analysis. For intensive subjects, frailty phenotyping was performed at screening, and cytokine and p16<sup>INK4a</sup> samples were not collected. Intensive subjects provided samples around a single observed dose; sparse sampling subjects provided samples on multiple occasions, ranging from a single occasion to three occasions. To accommodate outpatient visits during normal business hours in the research unit, dosing times for subjects with evening dose times were temporarily switched to morning dose times over several days of dose time adjustments. Subjects returned to estimated steady-state prior to sampling (5 to 7 days of dosing at the new dose time).

To be enrolled in the study, participants needed to demonstrate adherence, defined as <3 doses missed in the last 30 days, with no missed doses in the 3 days immediately prior to sampling report on provided dosing calendars. Subjects were asked to record the times of medication dosing for 7 days prior to the first visit, and for 3 days prior to subsequent study visits; actual dosing times were used in PK analysis. Participants with anemia by Division of Acquired Immunodeficiency Syndrome (National Institute of Allergy and Infectious Diseases, National Institutes of Health) grade 1 criterion (hemoglobin <10 mg/dL) unstable medical conditions, estimated creatinine clearance <30 mL/min as calculated by the Cockcroft-Gault formula using total body weight,<sup>30</sup> or Division of Acquired Immunodeficiency Syndrome grade 2 or higher laboratory abnormalities were excluded. Subjects receiving ATV/RTV were allowed to exceed this criterion for total bilirubin concentrations, if their clinician attributed this abnormality to the effects of the drug itself and deemed it clinically insignificant. Women of childbearing potential underwent urine pregnancy testing prior to providing samples at each visit to ensure samples were not collected from pregnant participants. CD4+ count and HIV viral load were obtained upon study initiation if they had not been collected for clinical purposes within 90 days of enrollment.

Fried frailty phenotyping<sup>20</sup> consisted of questions regarding unintentional weight loss, perceived effort of daily living, grip strength, walk time for 15 feet, and the Minnesota Leisure Activity Questionnaire. Each component has defined cutoff values, and if a subject's result for a component falls into the range defined as frail, this is a positive component. For example, if a subject's walk time exceeds the cutoff time based on height, this would be considered a positive component; if the time were less than the cutoff time, then it would be considered a negative component. Components are not weighted; the final result of this phenotyping is the sum of the positive components, and can range from 0–5. Frailty was defined as having three or more positive components of the phenotype; prefrail was defined as having one to two positive components; nonfrail was defined as having no positive components. Testing was conducted by staff of the NC TraCS Institute Bionutrition Core for consistency.

Only nonfrail participants age 55 or older were enrolled in the intensive sampling group (i.e., only older, nonfrail subjects were included in this group).

### Analytical methods

Total EFV, ATV, and RTV concentrations were analyzed using a validated liquid chromatography/ultraviolet detection method.<sup>31</sup> Complete assay range for EFV was 10–10,000 ng/mL, and 25–10,000 ng/mL for ATV and RTV, with inter- and intra-day coefficient of variation (CV)% ranged from 2.3–8.3%. Unbound EFV, ATV, and RTV concentrations were analyzed using rapid equilibrium dialysis and liquid chromatography tandem mass spectrometry. After thawing, samples were vortexed and underwent rapid equilibrium dialysis followed by protein precipitation. Stable, isotopically labeled EFV-d<sub>5</sub>, darunavir-d<sub>9</sub>, RTV-d<sub>6</sub> (in methanol) were used as internal standards. A Shimadzu 20AD series High Performance Liquid Chromatography System (Waters Corporation, Milford, MA) connected to an API 5000 MS/MS (AB Sciex Instruments, Framingham, MA) with a Waters Atlantis T3 column was used. Multiple reaction monitoring and positive mode were used for ATV/RTV; negative mode was used for EFV. Complete assay range for EFV was 0.25–5,000 ng/mL and 0.5–5,000 ng/mL for ATV and RTV. Overall assay precision and accuracy statistics met 15% acceptance criteria. All drug concentrations were determined in the UNC Center for AIDS Research Clinical Pharmacology and Analytical Chemistry Laboratory. The laboratory participates in national and international proficiency testing of its methods, and consistently achieves >95% accuracy in this testing.

Whole blood (7 mL), collected in K<sub>2</sub>EDTA tubes, was used to isolate CD3<sup>+</sup> T-cells and measure p16<sup>INK4a</sup> expression by Taqman quantitative reverse transcriptase-polymerase chain reaction using previously published methods in HIV-infected subjects.<sup>27</sup>

### Pharmacokinetic analysis

*Population pharmacokinetic modeling.* Population PK analyses of the drug concentration data were performed using NONMEM 7.3 (ICON Development Solutions, Hanover, MD). Data management, graphical analysis, and standard statistical analysis were conducted in R (version 3.1.0, r-project.org). Pirana (version 2.9.2) was used for model management and NONMEM output visualization. The ADVAN13 subroutine and stochastic approximation expectation maximization method were used for model development. For each drug, total and unbound concentrations were simultaneously described in one model, with the unbound concentration as the central compartment. The total drug concentrations were related to unbound drug with the unbound fraction,  $f_u$ .

For basic model selection, one-compartment and two-compartment models were tested for each drug. First-order input with or without a lag time and a mixture model were tested for the absorption. The effects of body weight and body mass index (BMI) on apparent unbound clearance (CL<sub>u</sub>/F) and apparent volume of distribution of unbound drugs (V<sub>u</sub>/F) were investigated as part of the structural model, using a power model and the empirical scaling factor, 0.75 and 1, for CL<sub>u</sub>/F and V<sub>u</sub>/F, respectively. Body

**Table 1** Participant demographics for each regimen

Characteristic	EFV arm (n = 60)	ATV/RTV arm (n = 31)
Age, years	48 (22–73)	49 (24–61)
HIV duration, years	10.5 (1–31)	10 (1–24)
BMI, kg/m <sup>2</sup>	27.2 (17.3–44.3)	30.3 (20.2–40.4)
CrCL, mL/min	108 (43–200)	100 (67–227)
Log <sub>2</sub> (p16 <sup>INK4a</sup> )	2.0 (0.20–2.8)	2.2 (0.16–3.9)
CD4 count, cells/mm <sup>3</sup>	662 (10–1,724)	692 (375–1,501)
Female	18 (30)	12 (39)
African American	34 (57)	19 (61)
White	22 (37)	10 (32)
Other race	4 (7)	2 (6)
Total frailty markers		
0	46 (77)	21 (68)
1–2	8 (13)	9 (29)
3	2 (3)	1 (3)
Phenotyping not completed	4 (7)	0 (0)

All participants received tenofovir disoproxil fumarate 300 mg and emtricitabine 200 mg by mouth once daily. Data are presented as median (range) or number (percentage).

ATV, atazanavir; BMI, body mass index; CrCL, creatinine clearance, as calculated by the Cockcroft-Gault equation; EFV, efavirenz; RTV, ritonavir.

weight was centered on 70 kg and BMI on 30 kg/m<sup>2</sup>. Those effects that decreased the objective function value by 3.84 ( $\alpha = 0.05$ ) were kept in the model. Interindividual variability (IIV) and interoccasional variability were assumed to be normally distributed and exponentially related to the population parameters. Proportional, additive, and combined proportional-additive error models were tested for residual variability, using the L2 data item to estimate correlation of this error for each drug. Model discrimination was determined by change in objective function value, using the likelihood ratio test ( $\alpha = 0.05$ ) and diagnostic plots.

### Covariate evaluation

The relationships of chronological age, p16<sup>INK4a</sup> expression, gender, race, body weight, BMI, the extent of frailty, and cytokine concentrations with PK parameter estimates were explored by graphical and standard statistical analysis. Continuous covariates were tested using correlation analysis and categorical variables using Wilcoxon rank sum tests ( $\alpha = 0.05$ ). Potential covariates were determined by their physiological possibilities and their relationships with the post hoc estimates of interindividual variability. Covariate analysis was performed using forward addition/backward elimination ( $\alpha = 0.05/0.01$ ). Besides the original continuous value, BMI was also converted to 0 or 1 split by 30 kg/m<sup>2</sup>. Categorical variables were incorporated using an exponential model, as shown below:

$$\theta = \theta_0 \times \theta_1^{COV_1} \times \theta_2^{COV_2} \times \dots \times \theta_i^{COV_i}$$

where  $\theta_0$  is the population parameter of the reference population,  $\theta_i$  is the fold change of parameter in the  $i$ th category from the reference,  $COV$  is the covariate of interest, and  $COV_i$  was assigned to 1 when the observation is within the  $i$ th category and otherwise 0.

Continuous variables were examined with proportional linear model (Eq. (1)), power model (Eq. (2)), or exponential model (Eq. (3)), as shown below.

$$\theta = \theta_1 \times [1 + \theta_2 \times (COV - \text{median}(COV))] \quad (1)$$

$$\theta = \theta_1 \times \left[ \frac{COV}{\text{median}(COV)} \right]^{\theta_2} \quad (2)$$

$$\theta = \theta_1 \times e^{\theta_2 \times [COV - \text{median}(COV)]} \quad (3)$$

Where  $\theta$  is the population PK parameter,  $\theta_1$  is the parameter of the population with the median  $COV$  value, and  $\theta_2$  is the covariate effect coefficient. Missing continuous covariates were imputed with the median value of the collected data, and missing categorical covariates were imputed as 0.

### Model validation

The goodness of fit of all models was evaluated by observation vs. individual prediction and population prediction plots, and normalized prediction distribution errors plots. Visual predictive checks were constructed with 1,000 simulations using the final parameter estimates to examine the prediction performance of the models, using the prediction-corrected visual predictive checks generated by Perl-Speaks-NONMEM (PsN).<sup>32</sup> Bootstrap estimates were obtained from 500 replicates generated by repeated random sampling of the original dataset with replacement, and were compared to model estimates to evaluate the precision of the parameter estimates.

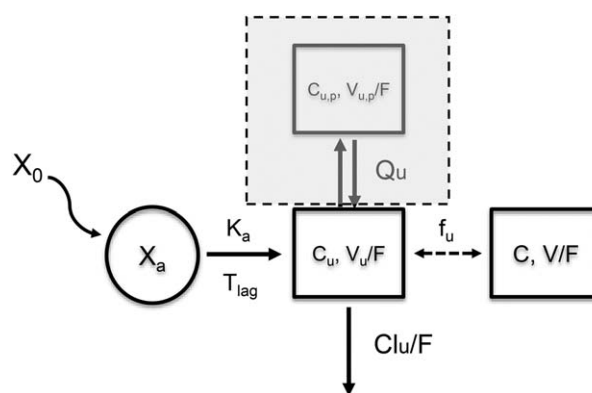


**Figure 1** Model schematics. The model for efavirenz and atazanavir includes the peripheral unbound plasma compartment, shown in the dashed box; the ritonavir model includes only the central compartment. The same basic structural model was used: first-order oral absorption with unbound plasma concentrations described by a linear model with unbound intrinsic clearance from the central compartment. Total drug concentrations were comodeled and linked to the unbound concentrations by the fraction unbound ( $f_u$ ), with total drug parameters as per the unbound structure models.  $CL_u/F$ , total oral clearance;  $CL_u/F$ , unbound oral clearance;  $f_u$ , fraction unbound of total drug;  $K_a$ , absorption rate constant;  $Q_u$ , intercompartmental clearance of total drug;  $Q_u/F$ , intercompartmental clearance of unbound drug;  $V/F$ , volume of total drug in the central compartment;  $V_p/F$ , volume of total drug in the peripheral compartment;  $V_{p,u}/F$ , volume of unbound drug in the peripheral compartment;  $V_u/F$ , volume of unbound drug in the central compartment.

**Table 2** Population pharmacokinetic estimates

Parameters (units)	ATV		RTV		EFV	
	Estimates (RSE%)	Bootstrap estimates (95% CI)	Estimates (RSE%)	Bootstrap estimates (95% CI)	Estimates (RSE%)	Bootstrap estimates (95% CI)
CL <sub>u</sub> /F (L/h)	101 (2)	105 (79.0–142)	772 * (3)	749 (566–962)	1,060 (1)	1,200 (982–1,410)
CL/F (L/h) <sup>a</sup>	5.73	–	4.85 *	–	6.93	–
V <sub>u</sub> /F (L)	1,110 (3)	1,090 (778–1,620)	8,430 * (2)	8,100 (5,380–10,900)	19,900 (1)	20,700 (14,800–29,700)
V/F (L) <sup>b</sup>	62.9	–	52.9 *	–	130	–
k <sub>a</sub> (h <sup>-1</sup> )	0.705 (42)	0.623 (0.452–0.885)	1.59 (32)	1.61 (1.19–2.47)	0.463 (5)	0.517 (0.382–0.653)
Lag time (h)	0.529 (36)	0.577 (0.165–1.10)	0.604 (51)	0.678 (0.323–0.873)	–	–
f <sub>u</sub> (%)	5.67 (1)	5.73 (5.34–6.11)	0.628 (1)	0.667 (0.551–0.782)	0.654 (0.5)	0.647 (0.621–0.681)
Q <sub>u</sub> /F (L/h)	134 (1)	137 (91.4–183)	–	–	5,940 (2)	3,980 (2,370–7,940)
Q/F (L/h) <sup>c</sup>	7.61	–	–	–	38.8	–
V <sub>p,u</sub> /F (L)	2,280 (1)	2,440 (1,730–2,950)	–	–	24,300 (1)	22,000 (18,600–28,400)
V <sub>p</sub> /F (L/h) <sup>d</sup>	129	–	–	–	159	–
Influence of BMI <30 on f <sub>u</sub> <sup>e</sup>	–	–	1.52 (1)	1.51 (1.22–2.00)	–	–
IIV (CV%)						
CL <sub>u</sub> /F	37.0 (1) [8%]	35.1 (26.4–44.0)	36.6 (3) [4%]	37.1 (20.4–54.4)	29.1 (1) [19%]	33.7 (6.91–51.9)
V <sub>u</sub> /F	44.3 (1) [14%]	42.3 (31.0–72.0)	75.4 (25) [2%]	80.8 (50.8–108)	68.6 (1) [19%]	47.1 (3.98–103)
k <sub>a</sub>	34.6 (1) [11%]	35.0 (20.0–54.5)	64 (17) [27%]	68.8 (26.7–137)	15.9 (3) [18%]	19.0 (3.12–67.4)
Lag time	80.6 (8) [19%]	77.0 (58.6–104)	120 (10) [24%]	128 (68.6–165)	–	–
f <sub>u</sub>	13.5 (4) [7%]	14.2 (9.1–18.5)	26.2 (17) [14%]	23.3 (11.2–34.6)	17.5 (14) [14%]	16.2 (9.54–22.4)
Q <sub>u</sub> /F	22.7 (14) [23%]	20.1 (3.82–54.6)	–	–	49.4 (8) [21%]	43.8 (6.66–143)
V <sub>p,u</sub> /F	22.6 (13.0) [30%]	19.8 (3.84–54.0)	–	–	31.9 (2) [19%]	17.7 (3.47–45.7)
IIV (CV%)						
CL <sub>u</sub> /F	73.9 (66)	69.2 (39.4–100)	60.5 (55)	58.0 (32.8–87.1)	42.4 (36)	44.0 (22.7–60.1)
Residual error (CV%)						
Total	27.6 (10)	27.8 (23.8–32.4)	41.4 (20)	45.5 (35.3–56.0)	24.2 (10)	24.9 (19.8–30.8)
Unbound	30.1 (11)	30.6 (26.9–34.8)	34.4 (33)	36.7 (28.7–45.7)	31.3 (20)	30.9 (25.1–37.0)

Shrinkage of IIV is indicated in brackets.

Data are presented as population means, residual SEs, and bootstrapped 95% CI; IIV, and residual variability are reported as CV%.

ATV, atazanavir; BMI, body mass index; CI, confidence interval; CL/F, apparent total clearance; CL<sub>u</sub>/F, apparent intrinsic clearance; CV, coefficient of variance; EFV, efavirenz; f<sub>u</sub>, unbound fraction; IIV, interindividual variability; k<sub>a</sub>, first order absorption rate constant; Q/F, apparent intercompartmental clearance of total drug; Q<sub>u</sub>/F, apparent intercompartmental clearance of unbound drug; RSE, relative standard error; RTV, ritonavir; V/F, apparent volume of distribution; V<sub>p</sub>/F, apparent peripheral volume of distribution; V<sub>p,u</sub>/F, apparent unbound peripheral volume of distribution; V<sub>u</sub>/F, apparent unbound volume of distribution.

<sup>a</sup>CL/F = CL<sub>u</sub>/F \* f<sub>u</sub>. <sup>b</sup>V/F = V<sub>u</sub>/F \* f<sub>u</sub>. <sup>c</sup>Q/F = Q<sub>u</sub>/F \* f<sub>u</sub>. <sup>d</sup>V<sub>p</sub>/F = V<sub>p,u</sub>/F \* f<sub>u</sub>. <sup>e</sup>f<sub>u</sub> = f<sub>u,POP</sub> \* COEF<sup>BMICAT</sup>, where f<sub>u,POP</sub> represents population estimate of unbound fraction with BMI >30 kg/m<sup>2</sup>, COEF is the covariate coefficient, BMICAT presents the BMI category with BMI >30 kg/m<sup>2</sup> classified as 0 and BMI <30 kg/m<sup>2</sup> as 1.

\*Population parameter estimates of subjects with body weight of 70 kg.

## Data exclusion

Outliers were determined using the residual plots from the final model. Observations yielding a ICWRESI >6 were considered as outliers and were excluded.

## RESULTS

### Participant disposition and demographics

For EFV, 60 subjects provided data for this analysis; 54 were sparsely sampled, and 6 provided intensive sampling. For ATV/RTV, 31 subjects provided data; 25 were sparsely sampled, and 6 provided intensive sampling. In addition to these drugs, all subjects also received tenofovir/emtricitabine 300/200 mg by mouth once daily. Participant demographics by regimen are presented in **Table 1**; demographics of the intensively sampled participants have been previously reported.<sup>28</sup> The median age in the EFV participants was 48 years, 18 were women, 8 demonstrated prefrailty, and 2

were frail. For the ATV/RTV participants, the median age was 49 years, 12 were women, 9 demonstrated prefrailty, and 1 was frail.

### Pharmacokinetic modeling

**Base model.** Model schematics for each drug are presented in **Figure 1**. No concentrations below the limits of quantification were measured for total drug; for ATV, one sample was below the limits of quantification, and for RTV, 9% of the samples were below the limits of quantification; half the lower limit of quantification was imputed as the concentration value. For EFV, one sample did not have sufficient volume for unbound analysis, and the same was true for five RTV samples; these concentrations were considered missing. The PK of unbound EFV was described using a two-compartment model with a first-order absorption phase. A lag time was not justified for EFV absorption, based on the change in objective function value. The PK of unbound ATV

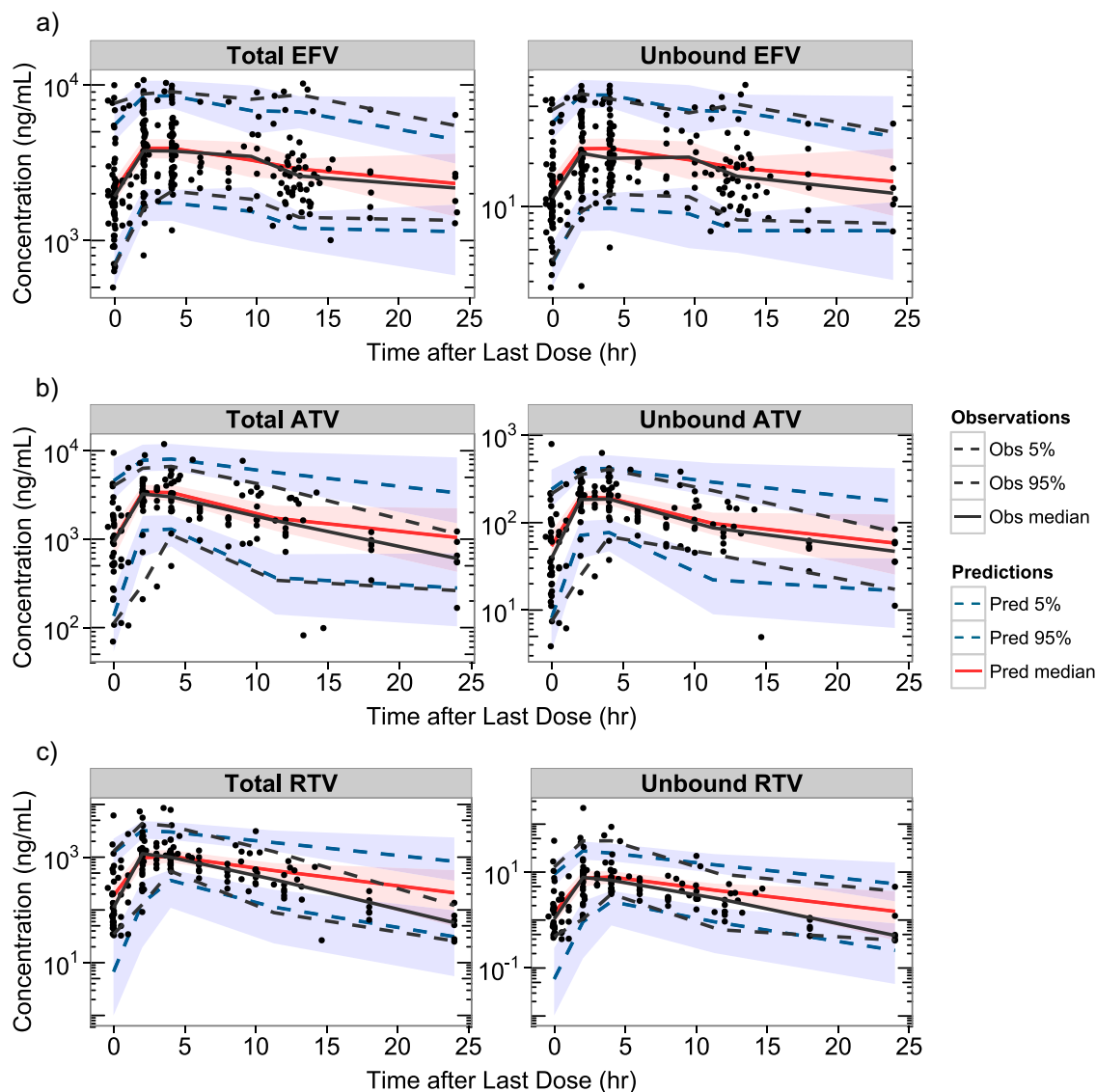


**Figure 2 (a–c)** Efavirenz (EFV), atazanavir (ATV), and ritonavir (RTV) prediction-corrected visual predictive checks for total (left) and unbound (right) drug. For each graph, time since the last dose in hours is on the x axis, with concentrations on the y axis. The black dots represent observed data. Percentiles of observations were presented in black, with solid lines for 50th percentiles and dotted lines for 5th and 95th percentiles. The 50th percentiles of predictions were presented in red solid lines, with 95% confidence intervals in red shaded areas. The 5th and 95th percentiles of predictions were presented in blue dotted lines, with 95% confidence intervals in blue shaded areas.

was described using a two-compartment model, following first-order absorption with a lag time. For RTV, a one-compartment model was sufficient, and the absorption phase was described using a first-order process with lag time. Empirical inclusion of the effects of body weight on apparent unbound clearance ( $CL_u/F$ ) and apparent volume of distribution ( $V_u/F$ ) was significant for RTV, but not for ATV or EFV. For ATV and RTV, due to mostly sparse sampling and a substantial variability in the absorption phase, the parameter estimates of the absorption rate constant ( $k_a$ ) and the lag time ( $T_{lag}$ ) were less precise than others, with their relative standard error  $>30\%$ . Interoccasional variability was incorporated on  $CL_u/F$  for the three drugs. The PK parameters of EFV were more precisely estimated compared to ATV and RTV, given a larger sample size. All the total and

unbound concentrations of the three drugs were included in the PK modeling analysis, with no outliers identified using the specified criteria. Parameter estimates for each model are presented in **Table 2**.

#### Covariate analysis

The exploratory analysis of *post hoc* estimates from the base models and covariates of interest showed relatively evident associations ( $P < 0.05$ ) between sex and RTV  $f_u$ , BMI and RTV  $f_u$ , but not other parameter-covariate pairs ( $P > 0.05$ ). Because the study was powered on aging-related factors, and  $CL_u/F$  and  $f_u$  were the parameters of most interest, covariate-parameter pairs involving chronological age,  $p16^{INK4a}$  expression, frailty phenotype, and scores,  $CL_u/F$  and  $f_u$  were further tested, along with the two pairs

mentioned above. Forward addition/backward elimination analysis supported the significant covariate effect of BMI on RTV  $f_u$ , either using BMI as a continuous or categorical variable. Using BMI as a categorical variable gave a more stable model in terms of parameter estimates and was therefore retained. Sex was not significant after the incorporation of BMI as a covariate. No other significant covariate effects of the other parameter-covariate pairs were found.

### Model validation

The diagnostic plots of EFV, ATV, and RTV indicate the model predictions correlate with the observations well, and there was no apparent bias in the models (**Supplementary Figures S1a–j, S2a–j, S3a–j**). The visual predictive checks of the three drugs (**Figure 2a–c**) demonstrated good performance of the models in predicting both total and unbound concentrations, with the predicted percentiles and corresponding 95% confidence intervals reasonably capturing the observed percentiles. Some overlap between prediction intervals near the end of the dosing interval are due to the sparsity of concentration data between 14–24 hours postdose.

## DISCUSSION

For the ARVs investigated here, the population total clearance and volume estimates for each drug are consistent with the literature,<sup>33–35</sup> and no significant covariate relationships with aging-related factors on unbound clearance or unbound fraction were demonstrated in HIV-infected subjects of a broad range of chronologic age. This is consistent with a previous analysis of associations of exposures with age, frailty phenotype, and p16<sup>INK4a</sup> expression.<sup>36</sup> In a study evaluating trough concentrations measured during therapeutic drug monitoring, their analysis suggested no changes in EFV concentrations with age, with increased concentrations of protease inhibitors, such as ATV and RTV, although only 16.5% of these participants were 50 years old or older.<sup>37</sup> In a noncompartmental analysis of ATV/RTV PK in Thai patients with HIV, age >42 years was found to be significantly associated with increased ATV and RTV area under the curve and peak plasma concentration ( $C_{max}$ ), however, the median age in this study was 42 years and the oldest subject was 57 years old.<sup>38</sup> In the present work, 38% of EFV and 36% of ATV/RTV participants were 50 years of age or older, with the oldest subject in each group 73 and 61, respectively. We believe this population analysis, with a higher number of older subjects, assessment of frailty and cellular senescence, and measurement of unbound drug supports current dosing strategies for older patients with HIV receiving EFV and ATV/RTV, as both total and unbound clearance do not appear to be altered here.

Because participants were enrolled at steady state, a thorough assessment of the central nervous system effects of EFV and their interaction with aging, where patients may be more susceptible to cognitive decline,<sup>39</sup> was not able to be done. Although unbound concentrations in plasma were not significantly higher in older participants, transport across the blood-brain barrier may be altered by age and inflammation.<sup>40,41</sup> Low numbers of frail participants may limit the

conclusions regarding changes in unbound clearance and protein binding; because participants were asked to provide four samples over one to two dosing intervals, some selection bias for frail participants is inherent. For EFV, the number of participants estimated to provide 90% power to detect age-related changes in clearance was exceeded, whereas the number of participants for ATV/RTV provided at least 80% power to detect age-related changes. Enrichment strategies to increase the frail participants in PK studies are ongoing, as well as pharmacogenomic analyses of these particular drugs to further explain IIV in model parameter estimates.

The analysis in this study suggests that the PK of RTV may be sensitive to body size. In the base model selection, the effects of body weight on RTV unbound clearance and volume of distribution of unbound are justified according to the objective function value, whereas this is not seen in the co-administrated protease inhibitor, ATV. This phenomenon is also observed on the unbound PK of RTV co-administrated with lopinavir in pregnancy.<sup>42</sup> In addition, the covariate analysis reveals the unbound fraction of RTV is 52% higher in participants with BMI <30 kg/m<sup>2</sup>, or 34% lower with BMI >30 kg/m<sup>2</sup>, implying participants who are moderately obese might have higher RTV protein binding. In the ATV/RTV group, female participants had a higher median BMI than the male participants, and both participants with BMI >40 were female. In this analysis, RTV protein binding was shown to be sensitive to BMI, but not ATV or EFV; in the PK literature, the relationship between obesity and protein binding has not been clearly delineated, although it is postulated that alpha-1 acid glycoprotein concentrations, to which RTV binds, are increased in obesity.<sup>43–45</sup> This may also be a function of sex differences, as BMI and sex are linked, and our sample size is moderate. Although the three frail participants had BMI values <30 kg/m<sup>2</sup>, no relationship between frailty and BMI was observed.

This work serves to highlight the importance of considering functional and immunologic assessments of age in assessing the PK of ARVs in the growing HIV-infected aging population, and conducting a thorough pharmacologic assessment of ARV disposition in adequate numbers of older participants. Although these drugs have fallen out of favor clinically in the United States,<sup>4</sup> given the advent of highly tolerable and effective integrase inhibitor regimens, this study design and the data generated add to the knowledge base of using ARVs in the growing population of aging HIV-infected patients, both domestically and globally.

**Acknowledgments.** The authors wish to thank the IRB 09-2120 study participants, as well as the staffs of the UNC Clinical and Translational Research Center (UL1RR02574), the UNC Health Care Infectious Diseases Clinic, and the Cone Health Regional Center for Infectious Diseases. We also thank Angela Kashuba for oversight of drug concentration analysis in the UNC Center for AIDS Research Clinical Pharmacology and Analytical Chemistry Laboratory. J.B.D. is supported by K23AI093156; funding for this work was provided in part by UL1RR02574 and the Society of Infectious Disease Pharmacists Young Investigator Research Award. M.C., H.M.A.P., C.S., N.W., S.M., and R.W. are supported in part by the UNC Center for AIDS Research (P30AI050410). C.T. and N.E.S. are supported by R01-AG024379-10.



**Conflict of Interest.** Noncompartmental analysis of the intensive study has been previously published (ref. 14). A statistical analysis of non-compartmental analysis of the sparse data has been previously published (ref. 15). C.T. is now an employee of Viiv Healthcare and owns stock in GlaxoSmithKline.

**Author Contributions.** J.B.D. and J.C. wrote the manuscript. J.B.D., H.M.A.P., K.B.P., and A.F. designed the research. J.B.D., M.C., C.R.T., H.M.A.P., and K.B.P. performed the research. J.B.D., J.C., M.C., C.R.T., C.S., C.T., N.W., S.M., R.W., N.E.S., and A.F. analyzed the data. N.E.S. contributed new reagents/analytical tools.

1. Klotz, U. Pharmacokinetics and drug metabolism in the elderly. *Drug Metab. Rev.* **41**, 67–76 (2009).
2. Benet, L.Z. & Hoener, B.A. Changes in plasma protein binding have little clinical relevance. *Clin. Pharmacol. Ther.* **71**, 115–121 (2002).
3. Butler, J.M. & Begg, E.J. Free drug metabolic clearance in elderly people. *Clin. Pharmacokinet.* **47**, 297–321 (2008).
4. Panel on Antiretroviral Guidelines for Adults and Adolescents. Guidelines for the use of antiretroviral agents in HIV-1-infected adults and adolescents. February 12, 2013, Department of Health and Human Services. <<https://aidsinfo.nih.gov/contentfiles/lvguidelines/adultandadolescentgl.pdf>>.
5. Effros, R.B. *et al.* Aging and infectious diseases: workshop on HIV infection and aging: what is known and future research directions. *Clin. Infect. Dis.* **47**, 542–553 (2008).
6. Centers for Disease Control and Prevention. HIV among people aged 50 and over. <<http://www.cdc.gov/hiv/group/age/olderamericans/index.html>>. Accessed 30 September 2016.
7. Bristol-Myers Squibb Company. Reyataz (atazanavir) Full U.S. prescribing information. Princeton, NJ. <[http://packageinserts.bms.com/pi/pi\\_evotaz.pdf](http://packageinserts.bms.com/pi/pi_evotaz.pdf)> (2009).
8. Klotz, U., Avant, G.R., Hoyumpa, A., Schenker, S. & Wilkinson, G.R. The effects of age and liver disease on the disposition and elimination of diazepam in adult man. *J. Clin. Invest.* **55**, 347–359 (1975).
9. Hanratty, C.G., McGlinchey, P., Johnston, G.D. & Passmore, A.P. Differential pharmacokinetics of digoxin in elderly patients. *Drugs Aging* **17**, 353–362 (2000).
10. Bristol-Myers Squibb Company. Sustiva (efavirenz) Full U.S. prescribing information. Princeton, NJ. <[http://packageinserts.bms.com/pi/pi\\_sustiva.pdf](http://packageinserts.bms.com/pi/pi_sustiva.pdf)> (2009).
11. Full U.S. prescribing information. Norvir (ritonavir) Tablets. AbbVie Inc. Revised September 2016. <<http://norvir.com/>>.
12. U.S. Food and Drug Administration. Guidance for industry: population pharmacokinetics. February 1, 1999. <<http://www.fda.gov/downloads/Drugs/GuidanceComplianceRegulatoryInformation/Guidances/ucm072123.pdf>> (1999).
13. Greenblatt, D.J., Divoll, M.K., Abernethy, D.R., Ochs, H.R., Harmatz, J.S. & Shader, R.I. Age and gender effects on chlorthalidone kinetics: relation to antipyrine disposition. *Pharmacology* **38**, 327–334 (1989).
14. Sotaniemi, E.A., Arranto, A.J., Pelkonen, O. & Pasanen, M. Age and cytochrome P450-linked drug metabolism in humans: an analysis of 226 subjects with equal histopathologic conditions. *Clin. Pharmacol. Ther.* **61**, 331–339 (1997).
15. Vestal, R.E., Norris, A.H., Tobin, J.D., Cohen, B.H., Shock, N.W. & Andres, R. Antipyrine metabolism in man: influence of age, alcohol, caffeine, and smoking. *Clin. Pharmacol. Ther.* **18**, 425–432 (1975).
16. Shi, S., Mörike, K. & Klotz, U. The clinical implications of ageing for rational drug therapy. *Eur. J. Clin. Pharmacol.* **64**, 183–199 (2008).
17. Alam, C., Whyte-Allman, S.K., Omeragic, A. & Bendayan, R. Role and modulation of drug transporters in HIV-1 therapy. *Adv. Drug Deliv. Rev.* **103**, 121–143 (2016).
18. Fu, Z.D., Csanaky, I.L. & Klaassen, C.D. Effects of aging on mRNA profiles for drug-metabolizing enzymes and transporters in livers of male and female mice. *Drug Metab. Dispos.* **40**, 1216–1225 (2012).
19. Schoen, J.C., Erlanson, K.M. & Anderson, P.L. Clinical pharmacokinetics of antiretroviral drugs in older persons. *Expert Opin. Drug Metab. Toxicol.* **9**, 573–588 (2013).
20. Fried, L.P. *et al.* Frailty in older adults: evidence for a phenotype. *J. Gerontol. A Biol. Sci. Med. Sci.* **56**, M146–M156 (2001).
21. Desquilbet, L. *et al.* HIV-1 infection is associated with an earlier occurrence of a phenotype related to frailty. *J. Gerontol. A Biol. Sci. Med. Sci.* **62**, 1279–1286 (2007).
22. Wynne, H.A., Cope, L.H., Herd, B., Rawlins, M.D., James, O.F. & Woodhouse, K.W. The association of age and frailty with paracetamol conjugation in man. *Age Ageing* **19**, 419–424 (1990).
23. Wynne, H.A., Yelland, C., Cope, L.H., Boddy, A., Woodhouse, K.W. & Bateman, D.N. The association of age and frailty with the pharmacokinetics and pharmacodynamics of metoclopramide. *Age Ageing* **22**, 354–359 (1993).

24. Groen, K. *et al.* The relationship between phenazone (antipyrine) metabolite formation and theophylline metabolism in healthy and frail elderly women. *Clin. Pharmacokinet.* **25**, 136–144 (1993).
25. Renton, K.W. Cytochrome P450 regulation and drug biotransformation during inflammation and infection. *Curr. Drug Metab.* **5**, 235–243 (2004).
26. Tsygankov, D. *et al.* A quantitative model for age-dependent expression of the p16INK4a tumor suppressor. *Proc. Natl. Acad. Sci. U. S. A.* **106**, 16562–16567 (2009).
27. Nelson, J.A. *et al.* Expression of p16(INK4a) as a biomarker of T-cell aging in HIV-infected patients prior to and during antiretroviral therapy. *Ageing Cell.* **11**, 916–918 (2012).
28. Dumond, J.B. *et al.* Pharmacokinetics of two common antiretroviral regimens in older HIV-infected patients: a pilot study. *HIV Med.* **14**, 401–409 (2013).
29. Bulitta, J.B., Bingölbali, A., Shin, B.S. & Landersdorfer, C.B. Development of a new pre- and post-processing tool (SADAPT-TRAN) for nonlinear mixed-effects modeling in S-ADAPT. *AAPS J.* **13**, 201–211 (2011).
30. Cockcroft, D.W. & Gault, M.H. Prediction of creatinine clearance from serum creatinine. *Nephron* **16**, 31–41 (1976).
31. Rezk, N.L., Tidwell, R.R. & Kashuba, A.D. High-performance liquid chromatography assay for the quantification of HIV protease inhibitors and non-nucleoside reverse transcriptase inhibitors in human plasma. *J. Chromatogr. B Analyt. Technol. Biomed. Life Sci.* **805**, 241–247 (2004).
32. Lindbom, L., Ribbing, J. & Jonsson, E.N. Perl-speaks-NONMEM (PsN)—a Perl module for NONMEM related programming. *Comput. Methods Programs Biomed.* **75**, 85–94 (2004).
33. Schipani, A. *et al.* Simultaneous population pharmacokinetic modelling of atazanavir and ritonavir in HIV-infected adults and assessment of different dose reduction strategies. *J. Acquir. Immune Defic. Syndr.* **62**, 60–66 (2013).
34. Dickinson, L. *et al.* Population pharmacokinetics of ritonavir-boosted atazanavir in HIV-infected patients and healthy volunteers. *J. Antimicrob. Chemother.* **63**, 1233–1243 (2009).
35. Csajka, C. *et al.* Population pharmacokinetics and effects of efavirenz in patients with human immunodeficiency virus infection. *Clin. Pharmacol. Ther.* **73**, 20–30 (2003).
36. Dumond, J.B. *et al.* Tenofovir/emtricitabine metabolites and endogenous nucleotide exposures are associated with p16(INK4a) expression in subjects on combination therapy. *Antivir. Ther.* **21**, 441–445 (2016).
37. Winston, A. *et al.* Effects of age on antiretroviral plasma drug concentration in HIV-infected subjects undergoing routine therapeutic drug monitoring. *J. Antimicrob. Chemother.* **68**, 1354–1359 (2013).
38. Avihingsanon, A. *et al.* Short communication: Aging not gender is associated with high atazanavir plasma concentrations in Asian HIV-infected patients. *AIDS Res. Hum. Retroviruses* **29**, 1541–1546 (2013).
39. John, M.D. *et al.* Geriatric assessments and association with VACS index among HIV-infected older adults in San Francisco. *J. Acquir. Immune Defic. Syndr.* **72**, 534–541 (2016).
40. Varatharaj, A. & Galea, I. The blood-brain barrier in systemic inflammation. *Brain Behav. Immun.*; e-pub ahead of print 2016.
41. Marques, F., Sousa, J.C., Sousa, N. & Palha, J.A. Blood-brain-barriers in aging and in Alzheimer's disease. *Mol. Neurodegener.* **8**, 38 (2013).
42. Chen, J., Malone, S., Prince, H.M., Patterson, K.B. & Dumond, J.B. Model-based analysis of unbound lopinavir pharmacokinetics in HIV-infected pregnant women supports standard dosing in the third trimester. *CPT Pharmacometrics Syst. Pharmacol.* **5**, 147–157 (2016).
43. Benedek, I.H., Fiske, W.D. 3rd, Griffen, W.O., Bell, R.M., Blouin, R.A. & McNamara, P.J. Serum alpha 1-acid glycoprotein and the binding of drugs in obesity. *Br. J. Clin. Pharmacol.* **16**, 751–754 (1983).
44. Benedek, I.H., Blouin, R.A. & McNamara, P.J. Serum protein binding and the role of increased alpha 1-acid glycoprotein in moderately obese male subjects. *Br. J. Clin. Pharmacol.* **18**, 941–946 (1984).
45. Blouin, R.A., Kolpek, J.H. & Mann, H.J. Influence of obesity on drug disposition. *Clin. Pharm.* **6**, 706–714 (1987).

© 2016 The Authors CPT: Pharmacometrics & Systems Pharmacology published by Wiley Periodicals, Inc. on behalf of American Society for Clinical Pharmacology and Therapeutics. This is an open access article under the terms of the Creative Commons Attribution-NonCommercial-NoDerivs License, which permits use and distribution in any medium, provided the original work is properly cited, the use is non-commercial and no modifications or adaptations are made.

Supplementary information accompanies this paper on the *CPT: Pharmacometrics & Systems Pharmacology* website (<http://psp-journal.com>)